



NRC Publications Archive Archives des publications du CNRC

Thermal decomposition of nanoparticulate Ca(OH)₂ - anomalous effects

Sato, T.; Beaudoin, J. J.; Ramachandran, V. S.; Mitchell, L. D.; Tumidajski, P. J.

This publication could be one of several versions: author's original, accepted manuscript or the publisher's version. / La version de cette publication peut être l'une des suivantes : la version prépublication de l'auteur, la version acceptée du manuscrit ou la version de l'éditeur.

Publisher's version / Version de l'éditeur:

Advances in Cement Research, 19, January 1, pp. 1-7, 2007-01-01

NRC Publications Record / Notice d'Archives des publications de CNRC:

<https://nrc-publications.canada.ca/eng/view/object/?id=8944af28-79bd-40e3-a2fc-446de25b9d66>
<https://publications-cnrc.canada.ca/fra/voir/objet/?id=8944af28-79bd-40e3-a2fc-446de25b9d66>

Access and use of this website and the material on it are subject to the Terms and Conditions set forth at

<https://nrc-publications.canada.ca/eng/copyright>

READ THESE TERMS AND CONDITIONS CAREFULLY BEFORE USING THIS WEBSITE.

L'accès à ce site Web et l'utilisation de son contenu sont assujettis aux conditions présentées dans le site

<https://publications-cnrc.canada.ca/fra/droits>

LISEZ CES CONDITIONS ATTENTIVEMENT AVANT D'UTILISER CE SITE WEB.

Questions? Contact the NRC Publications Archive team at

PublicationsArchive-ArchivesPublications@nrc-cnrc.gc.ca. If you wish to email the authors directly, please see the first page of the publication for their contact information.

Vous avez des questions? Nous pouvons vous aider. Pour communiquer directement avec un auteur, consultez la première page de la revue dans laquelle son article a été publié afin de trouver ses coordonnées. Si vous n'arrivez pas à les repérer, communiquez avec nous à PublicationsArchive-ArchivesPublications@nrc-cnrc.gc.ca.



NRC-CNRC

*Institute for
Research in
Construction*

CNRC-NRC

*Institut de
recherche en
construction*

<http://irc.nrc-cnrc.gc.ca>

Thermal decomposition of nanoparticulate Ca(OH)₂-anomalous effects

NRCC-45602

Sato, T.; Beaudoin, J.J.; Ramachandran,
V.S.; Mitchell, L.D.; Tumidajski, P.J.

A version of this document is published in
/ Une version de ce document se trouve
dans: *Advances in Cement Research*, v.
19, no. 1, Jan. 2007, pp. 1-7



National Research
Council Canada

Conseil national
de recherches Canada

Canada

Thermal Decomposition of Nanoparticulate Ca(OH)₂-Anomalous Effects

T.Sato* , J. J. Beaudoin.*, V. S.Ramachandran*, L. D.Mitchell*, and P.J. Tumidajski**

ABSTRACT

Different forms of Ca(OH)₂ with varying degrees of crystallinity and surface area were prepared using Ca(OH)₂ and CaCO₃ as starting materials. They were decomposed and the hydrated CaO formed at different conditions. The nitrogen surface area values of Ca(OH)₂ ranged from 3.7 to 31.1 m²/g. The presence of two separate and distinct thermal decomposition events (in DTG) was observed, depending on the degree of crystallinity. Endotherms occurred at temperatures of about 426 and 454°C. Binary mixtures of Ca(OH)₂ with substantially different degrees of crystallinity exhibited a well defined thermal decomposition doublet. The peak height of each endotherm was dependent on the mass proportions of each mixture component. Factors, including thermodynamic considerations, affecting the character of the decomposition behavior of Ca(OH)₂ are discussed.

*Institute for Research in Construction, National Research Council of Canada, Ottawa
Canada, K1A0R6

** Centre for Advanced Building Technologies, The City College George Brown,
Toronto, Canada, M5T 2T9

Introduction

Calcium hydroxide (CH) forms a significant fraction of the volume occupied by the products formed by the hydration of the silicate components of the cement. The range of CH contents in well-cured Portland cement pastes has been reported to vary from 15 to 25% (ignited weight basis)¹. It has been suggested that the presence of nanometer-scale CH is, at the most, limited in amount². There appears to be no evidence for the presence of amorphous or cryptocrystalline CH (except in paste formed at low water-solid ratios) in cement pastes.

The role of CH in cement-based materials is multifaceted. It is a reactant in many reactions that impact the durability of cement paste and concrete³. These include chemical resistance, alkali-aggregate reactions, leaching, efflorescence and, for example, chemical processes related to sulfate attack and carbonation. Calcium hydroxide, however, provides protection against the corrosion of steel in concrete and protects the C-S-H phase. The engineering properties of CH itself are similar to those of the C-S-H⁴. For example, the fracture mechanics parameter, K_c (the critical stress intensity factor), for C-S-H and mixtures of C-S-H and CH increases co-linearly with the polymer/dimer ratio of the C-S-H. The CH can also have a significant influence on the hydration chemistry of cement systems containing pozzolans and reactions involving cement minerals themselves e.g. C_3A and AF_t phases⁵.

The above commentary underscores the importance of analytical techniques for identification and quantification of this important component of cement and concrete products. Monitoring of the thermal decomposition of CH in cement pastes by DTA, DSC and TG methods enables its estimation⁶⁻⁹. Factors that affect the character of the decomposition events in any of the related spectra are of importance to cement chemistry. Greene reported on the double character of the peaks (DTA curves of Portland cement hydrated for various lengths of time) in the vicinity of 500°C¹⁰. He suggested the possibility that the first endotherm in this region represented chemisorbed water held on the surface of free lime particles. The second larger peak was attributed to the more coarsely crystalline calcium hydroxide formed by precipitation from solution. Herrick et al. reported the presence of a doublet (for a similar temperature range) in their DTA traces of hydrating expansive clinker pastes¹¹. The lower temperature peak was attributed to the presence of metastable cubic CH pseudomorphs. Slow decomposition to the hexagonal form of CH accounted for the second higher temperature peak. It was thought that the doublet could be due to the existence of CH of different surface areas.

The results of a systematic study designed to investigate the synthesis of high surface area nanoparticulate CH and the nature of its thermal decomposition are reported in this paper. The nature of the thermal decomposition doublet (in the 500°C range) is described. High surface area CH is important in the context of nanoscience as it relates to cement chemistry.

Experimental

Materials

CaO: Calcium oxide was prepared as described in Table 1.

Ca(OH)₂: Eight different samples of Ca(OH)₂ were prepared. The procedures are described in Table 2.

LiCl and NaCl: These reagent grade salts were used to prepare saturated solutions for humidity control, LiCl (11%RH) and NaCl (75%RH). The former was supplied by Fisher Scientific, New Jersey, USA and the latter by E.M. Darmstadt Germany.

TG/DSC

The TG and DSC measurements were obtained using a simultaneous DSC-TG instrument-a TA Instruments SDT-Q600 Thermal Analyzer. A heating rate of 10°C/min (room temperature to 1050°C) in a nitrogen gas environment (100 mL/min) was employed. Results for TG are plotted in a derivative form (DTG). Results from DSC measurements (heat flow data) were used for heat capacity calculations.

XRD

X-ray diffraction measurements were taken using a Scintag XDS 2000 instrument. CuK α radiation (45KV, 35mA) was used. The scan rate was 0.025 degrees/sec. The spectra were obtained in the interval 5° < 2 θ < 85°.

BET

Nitrogen surface area measurements were obtained with a Quantachrome Quantasorb Sorption System. Samples were dried using a heating mantle at 140°C for 10 minutes prior to the measurements. The surface area values are provided in Table 3.

Results and Discussion

The study was initiated to investigate methods of preparation of high surface area CH and the characteristics of its thermal decomposition.

The DTG results for samples CH-1 and CH-2 and their mixtures with different proportions are presented in Figure 1. The decomposition peaks for the single component samples occur at 426°C for CH-1 and 454°C for CH-2. Well-defined doublets appear for the blended samples consistent with the variation in content of each sample. The sample CH-2, liquid-hydrated, has a significantly higher decomposition temperature than the vapor-hydrated CH-1. The series of DTG results for CH-1 and CH-6 show similar trends (see Figure 2). There are two separate and distinct thermal decomposition endotherms for the two samples. The CH-2 and CH-6 samples have similar decomposition characteristics despite the large difference in surface area (31.1 compared to 7.3 m²/g). Both these samples were produced by liquid hydration. The vapour-hydrated CH-1 preparation (20.1 m²/g) had the lowest decomposition temperature. The high surface area samples (CH-1 and CH-2) have a lower average particle size than the low surface area sample (CH-6), (see SEM micrographs, Figure 3). The effect of vapour hydration at high humidity (75%RH) as opposed to low humidity (11%RH) was also evaluated. Hydration of CaO

produced by decomposition of calcium hydroxide at 600°C was accelerated at 75%RH. The reaction (as determined by TGA) went to completion in 3 hours. The DTG results for mixtures of this reaction product, CH-3, and the high surface area material, CH-2, display the characteristic doublets described above, Figure 4. Mixtures of the reagent grade calcium hydroxide, CH-4, and CH-2 also produce doublets in the DTG plots (not shown). The difference in the peak decomposition temperature of these samples is not as pronounced as that between CH-1 and CH-2. Factors affecting the decomposition temperature of CH are discussed as follows:

Particle Size and Crystallinity:

It might be expected that decomposition temperature would be dependent on particle size i.e. the lower the particle size the lower the temperature of decomposition. This is the case for particles of pyrites (200-2 μ m) where the peak temperature decreased by about 100°C [12]. Results of studies, however, on the effect of particle size are often conflicting. Unusual effects such as the development of new peaks and disappearance of the normal peaks owing to the destruction of the lattice itself can occur. Differences attributed in many instances to the particle size may in fact be due to the lower degree of crystallinity [13]. For example, grinding CaCO₃ for prolonged periods may destroy the crystallinity and decompose the material. Further, grinding dolomite reduces the particle size and almost completely eliminates the decomposition peak [14]. The effect of degree of crystallinity can be better understood by crushing CaCO₃ to any required particle size without destroying the crystallinity [15]. There appears to be no particle size effect in this system if the degree of crystallinity of the particles is similar.

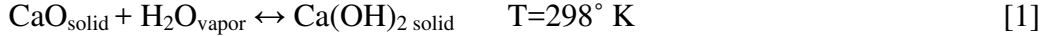
X-ray Diffraction Analysis:

It is suggested that differences in decomposition temperature of the CH observed in this study are due to differences in crystallinity. Crystallinity determined by the XRD analysis is mainly affected by crystallite size and strain. In addition, there is an instrumental error associated with the XRD peaks. Therefore, the XRD analysis only indicates crystallinity of material indirectly. However, in order to compare the results with works by other researchers, the following method for the calculation of crystallinity index from XRD spectra was conducted. The inverse of the peak width at half peak height (e.g. at $2\theta = 34.09^\circ$) from the baseline was taken as an indicator of the crystallinity. Values for crystallinity index and thermal decomposition temperature are given in Table 4. Higher values of the crystallinity index indicate a higher degree of crystallinity. The view that the on-set of decomposition temperature is dependent on the degree of crystallinity and not particle size is supported by the data. This view is also consistent with the work of Bayliss who determined that the thermal decomposition of high purity CaCO₃ was independent of particle size [15,16]. In addition to the crystallinity index estimates, Williamson-Hall plots were constructed from the X-ray data using Bruker AXS.TOPAS V2.1 software [17]. It was shown that line broadening can be attributed to simultaneous strain and small particle size broadening [18]. The plots of $B\cos\theta$ versus $\sin\theta$ are linear with the intercepts providing semi-quantitative values of the volume weighted characteristic length $\langle L \rangle_{vol}$ and the slopes indicating the level of lattice

strain. The software enables the ‘B’ term to be extracted from the ‘full width-half maximum’ values (FWHM) of ‘double-Voigt’ fitting to the sample and the LaB₆ standard. The magnitude of the slopes of the lines and the degree of disorder are in the following order, CH-1 > CH-2 > CH-6, indicating that the lower decomposition temperature would be expected for the CH-1 preparation.

Thermodynamic Considerations:

Consider the reaction of CaO_{solid} with water vapor, H₂O_{vapor} at 25°C (298°K).



It can be demonstrated (see appendix 1) that ΔG , the change in Gibbs Free Energy for the reaction becomes more negative as relative humidity increases (i.e. the thermodynamic driving force for the reaction increases). A more negative value of ΔG also corresponds to a more stable CH product. This is consistent with a variation in the decomposition temperature of CH observed in the DTG analysis. More direct evidence for this statement is provided by the heat capacity (C_p) data analysis for the CH preparations where the heat capacity of the CH formed under different hydration conditions is determined as a function of temperature.

The heat capacities were calculated using the equation,

$$\left(\frac{Q}{m}\right) = C_p \cdot \left(\frac{\partial T}{\partial t}\right) = (\text{W g}^{-1}) = (\text{J s}^{-1} \text{g}^{-1}) = (\text{J g}^{-1} \text{ } ^\circ\text{K}^{-1}) \cdot (^\circ\text{K s}^{-1}) \quad [2]$$

where,

Q is the applied power (Watts or Joules per second),

m is the sample mass (grams),

C_p is the heat capacity (Joules per gram per degree Kelvin),

$\left(\frac{\partial T}{\partial t}\right)$ is the heating rate (degrees Kelvin per second).

The results are summarized in Figure 5 in the 298-675° K temperature range. The reference value from Kubaschewski and Alcock has also been included in Figure 5 for comparison [19].

There are a number of relevant features in Figure 5. In the range 310° to 350° K, there is a discontinuity in the heat capacity (C_p) curve with a sharp maximum at 328° K. This behaviour indicates a transformation [20]. For the present results, the C_p behaviour is most likely a displacive transition similar to the ferroelectrics with perovskite or ilmenite ionic crystal structures [21]. At the higher temperatures, the C_p curves, sharply and asymptotically approach the dissociation temperature, T_d , of the Ca(OH)₂ wherein the Ca(OH)₂ dissociates to CaO and H₂O_{vapor}. The T_d of the Ca(OH)₂ depends on the temperature and method of preparation. In agreement with the results of other parts of this study, water hydration and higher temperatures of preparation, increases the T_d of the

Ca(OH)₂. The observation is further evidence suggesting the presence of different allotropes of Ca(OH)₂ depending on the temperature and method of hydration of CaO.

The heat capacity C_p varies monotonically with temperature between 350 °K and 500 °K,. The relationships are indicated in Figure 6. It can be seen that the temperature dependence for the literature values of Ca(OH)₂ are not as strongly dependent on temperature as are the C_p values determined in this study.

Conclusions

1. Two or more distinct forms of calcium hydroxide with separate thermal decomposition temperatures (doublets) can easily be produced.
2. Calcium hydroxide preparations of varying crystallinity can be produced by employing vapor phase and liquid phase hydration of CaO.
3. Thermal decomposition temperatures of calcium hydroxide are not necessarily dependent on surface area or particle size. They appear related more to the degree of crystallinity.
4. Previously observed doublets (in the vicinity of 500°C) in the DTA spectra of hydrated cement systems can be explained on the basis of differences in crystallinity of Ca(OH)₂ produced in cements under certain conditions that involve the type of cement and hydration environment.
5. Thermodynamic calculations based on Gibbs Free Energy changes and heat capacity data are in accord with the observed differences in the decomposition temperature for CH preparations.

References

1. Taylor H.F.W., Cement Chemistry, 2nd edition, Thomas Telford, London, 1997.
2. Diamond S., Calcium hydroxide in cement paste and concrete- a microstructural appraisal. Materials Science of Concrete, Special Volume: Calcium Hydroxide in Concrete, Vol. 6, edited by J. Skalny, J. Gebauer, J. Odler, Amer. Ceram. Soc., Westerville, 2001, pp.37-58.
3. Glasser F. P., The role of Ca(OH)₂ in Portland cement concretes. *ibid*, 2001, pp.11-36
4. Beaudoin J. J., Gu P., Myers R. E., The fracture of C-S-H and C-S-H/CH mixtures *Cem. Concr. Res.* 1998 ,**28**, 341-347.

5. Brown P. and Clark B., An overview of the role of $\text{Ca}(\text{OH})_2$ in cementing systems., *ibid*, 2001, **31**, 73-75.
6. Ramachandran V.S., Differential thermal method of estimating calcium hydroxide in calcium silicate and cement phases. *Cem. Concr. Res.* 1979, **9**, 677-684.
7. Ramachandran V.S., Feldman R. F. and Sereda P.J., Applications of thermal analysis in cement research. *Highway Res. Rec.*, 1964, **62**, 40-61.
8. Ramachandran V.S. and Polomark G. M., Extraction of $\text{Ca}(\text{OH})_2$ from Portland cement and $3\text{CaO} \cdot \text{SiO}_2$ pastes. *J. Chem. Tech. And Biotech.*, 1982, **32**, **946-952**.
9. Butler F. G. and Morgan S. R., A thermoanalytical method for determination of the amount of $\text{Ca}(\text{OH})_2$ contained in hydrated Portland cement. *Proc. 7th Int. Congr. Chem. Cem.*, Paris, 1980, Vol. II, pp.43-46.
10. Greene K. T., Early hydration reactions of Portland cement. *Proc. 4th Int. Cong. Chem. Cem.*, Washington D.C., 1962, Session IV, Paper-IV-1, pp.359-374.
11. Herrick J., Scrivener K. and Pratt P., The development of microstructure in calcium sulphoaluminate expansive cement. *Proc. Matls. Res. Soc.*, Pittsburgh Pa. 1992, Vol 245, pp.277-282.
12. Polizzotti C. and Grillone M. D., Determinazione quantitativa della pirite con l'analisi termica differenziale, *Ann. Chem. (Roma)*, 1963, **53** 1476.
13. Tanaka T., Simultaneous grinding and reaction. *Minerals Process*, 1964, **5**, 31.
14. Barta R., Bruthans Z., Effect of grinding on the structure of crystalline substances investigated by differential thermal analysis. *Proc. 6th Conf Silicate Ind.*, Budapest, 1961, pp.17-28.
15. Bayliss P., Effect of particle size on differential thermal analysis. *Nature*, 1964, **201**, 1019.
16. Ramachandran V. S., Applications of differential thermal analysis in cement chemistry . *Chem. Pub. Co.*, N.Y., 1969, pp308.
17. Bruker AXS. TOPAS V2.1 user manual, Karlsruhe Germany, 2003.
18. Williamson G.K. and Hall W.H., X-Ray line broadening from fided aluminium and wolfram.. *Acta Metallurgica* 1953, **1**, 22-31.
19. Kubaschewski O. and Alcock C. B. Metallurgical thermochemistry. 5th edition

Pergamon Press, Toronto,1979, p.342.

20. Ibid,pp.11-12.
21. Kittel C. Introduction to solid state physics 6th edition, Wiley, New York, 1986, pp.372-384.

Table 1 Preparation of CaO

	Preparation
CaO-1	Reagent grade calcium hydroxide was heated to 600°C and held isothermally for 1 hour. The nitrogen surface area of CaO was 31.2 m ² /g.
CaO-2	Reagent grade calcium carbonate was heated to 1050°C and held isothermally for 1 hour. The nitrogen surface area of CaO was 2.6 m ² /g.
CaO-3	Reagent grade calcium carbonate was heated to 1400°C and isothermally held for 1 hour. The nitrogen surface area of CaO was 1.9 m ² /g.

Table 2 Methods of Preparation of Calcium Hydroxide Samples

Sample	Preparation
CH-1	CaO-1 was hydrated in an 11%RH environment for 7 days.
CH-2	CaO-1 was hydrated in deaerated water for 7 days.
CH-3	CaO-1 was hydrated in a 75% RH environment for 3 hours.
CH-4	Reagent grade Ca(OH) ₂
CH-5	CaO-2 was hydrated in an 11% RH environment for 7 days

CH-6	CaO-2 was hydrated in deaerated water for 7 days.
CH-7	CaO-3 was hydrated in an 11%RH environment for 7 days.
CH-8	CaO-3 was hydrated in deaerated water for 7 days.

Table 3 BET surface area values for various Ca(OH)₂ preparations

Sample	CH-1	CH-2	CH-3	CH-4	CH-5	CH-6	CH-7	CH-8
Surface Area, m ² /g	20.1	31.1	21.5	16.6	3.7	7.3	5.1	7.8

Table 4 Characterization data for selected CH preparation

Sample	BET, m ² /g	Crystallinity Index	Decomp. Onset, (1)	Decomp. Peak	Decomp. End, (2)	(2) – (1)
CH-1	20.1	1.72	231°C	426°C	467°C	236°C
CH-2	31.1	3.03	299°C	454°C	511°C	212°C
CH-6	7.3	5.26	308°C	452°C	512°C	204°C

LIST OF FIGURES

Figure 1: DTG curves for samples CH-1 and CH-2 and their mixtures with different proportions

Figure 2: DTG curves for samples CH-1 and CH-6 and their mixtures with different proportions

Figure 3: SEM micrographs of CH-1, CH-2 and CH-6

Figure 4: DTG curves for samples CH-3 and CH-2 and their mixtures with different proportions

Figure 5: Temperature dependence of heat capacities for Ca(OH)₂ prepared under different conditions.

Figure 6: Region of linear temperature dependence for Ca(OH)₂ heat capacities.

APPENDIX 1

Consider the reaction of $\text{CaO}_{(\text{solid})}$ with water vapour, $\text{H}_2\text{O}_{(\text{vapor})}$ at 25°C (298°K).



$$[1] \quad \Delta H_{\text{Reaction}, 298 \text{ K}}^\circ = \Delta H_{\text{Formation}, \text{Ca}(\text{OH})_{2(\text{solid})}}^\circ - \Delta H_{\text{Formation}, \text{CaO}_{(\text{solid})}}^\circ - \Delta H_{\text{Formation}, \text{H}_2\text{O}_{(\text{vapor})}}^\circ$$

$$[2] \quad \Delta H_{\text{Reaction}, 298 \text{ K}}^\circ = -235,500 - (-151,600) - (-57,795) = -26,105 \text{ calories mol}^{-1}$$

$$\Delta S_{\text{Reaction}, 298 \text{ K}}^\circ = S_{\text{Formation}, \text{Ca}(\text{OH})_{2(\text{solid})}}^\circ - S_{\text{Formation}, \text{CaO}_{(\text{solid})}}^\circ - S_{\text{Formation}, \text{H}_2\text{O}_{(\text{vapor})}}^\circ$$

$$[3] \quad \Delta S_{\text{Reaction}, 298 \text{ K}}^\circ = 19.93 - (9.5) - (45.106) = -34.68 \text{ calories mol}^{-1} \text{ }^\circ\text{K}^{-1}$$

Substituting Eq.[2] and [3] into the Gibbs-Helmholtz equation gives,

[4]

$$\Delta G_{\text{Reaction}, 298 \text{ K}}^\circ = \Delta H_{\text{Reaction}, 298 \text{ K}}^\circ - T \cdot \Delta S_{\text{Reaction}, 298 \text{ K}}^\circ = -26,105 - (298) \cdot (-34.68) = -15,769 \text{ calories mol}^{-1}$$

The $^\circ$ notation indicates that all components are in their standard states. In this case, the activities of solids are one, and the pressure of gases will be 1 atm. The generalized version of Eq.[4] for conditions other than the standard state is given by,

$$[5] \quad \Delta G_{\text{Reaction}, T} = \Delta G_{\text{Reaction}, T}^\circ + R \cdot T \cdot \ln \left(\frac{a_{\text{Ca}(\text{OH})_{2(\text{solid})}}}{a_{\text{CaO}_{(\text{solid})}} \cdot P_{\text{H}_2\text{O}_{(\text{vapor})}}} \right)$$

For the present situation,

$$T = 298 \text{ K}$$

$$R = \text{universal gas constant} = 1.987 \text{ calories mol}^{-1} \text{ }^{\circ}\text{K}^{-1}$$

$$a_{\text{Ca(OH)}_2(\text{solid})} = \text{activity of solid Ca(OH)}_2 = 1$$

$$a_{\text{CaO}(\text{solid})} = \text{activity of solid CaO} = 1$$

$$P_{\text{H}_2\text{O}(\text{vapor})} = \text{normalized partial pressure of water vapor present}$$

At 298 K, the equilibrium normalized H₂O vapour pressure is,

$$P_{\text{H}_2\text{O}(\text{vapor})}^{\text{equilibrium}} = \frac{3.17 \text{ kPa}}{101.3 \frac{\text{kPa}}{\text{atm}}} = 0.0313 \text{ atm}$$

For an 11% relative humidity at 298 K, this means,

$$[6] \quad P_{\text{H}_2\text{O}(\text{vapor})}^{11\% \text{ RH}} = 0.11 \times 0.0313 = 0.0034 \text{ atm}$$

Therefore, substituting Eq.[4] and [6] into Eq.[5] and with the values for the activities of the solid phases set to one, yields

$$[7] \quad \Delta G_{\text{Reaction}, 298 \text{ K}}^{11\% \text{ RH}} = -15,769 - 592 \ln(0.0034) = -12,404 \text{ calories mol}^{-1}$$

Similar calculations for 75% relative humidity at 298 K, gives

$$[8] \quad \Delta G_{\text{Reaction}, 298 \text{ K}}^{75\% \text{ RH}} = -15,769 - 592 \ln(0.0235) = -13,548 \text{ calories mol}^{-1}$$

The results shows that at 298 K, there is a greater driving force when CaO is vapor hydrated at 75% relative humidity compared to 11% relative humidity. Since

$$\Delta G_{\text{Reaction}, 298 \text{ K}}^{75\% \text{ RH}} < \Delta G_{\text{Reaction}, 298 \text{ K}}^{11\% \text{ RH}}, \text{ this suggests the Ca(OH)}_2 \text{ produced at 75\% relative}$$

humidity may be more thermodynamically stable.

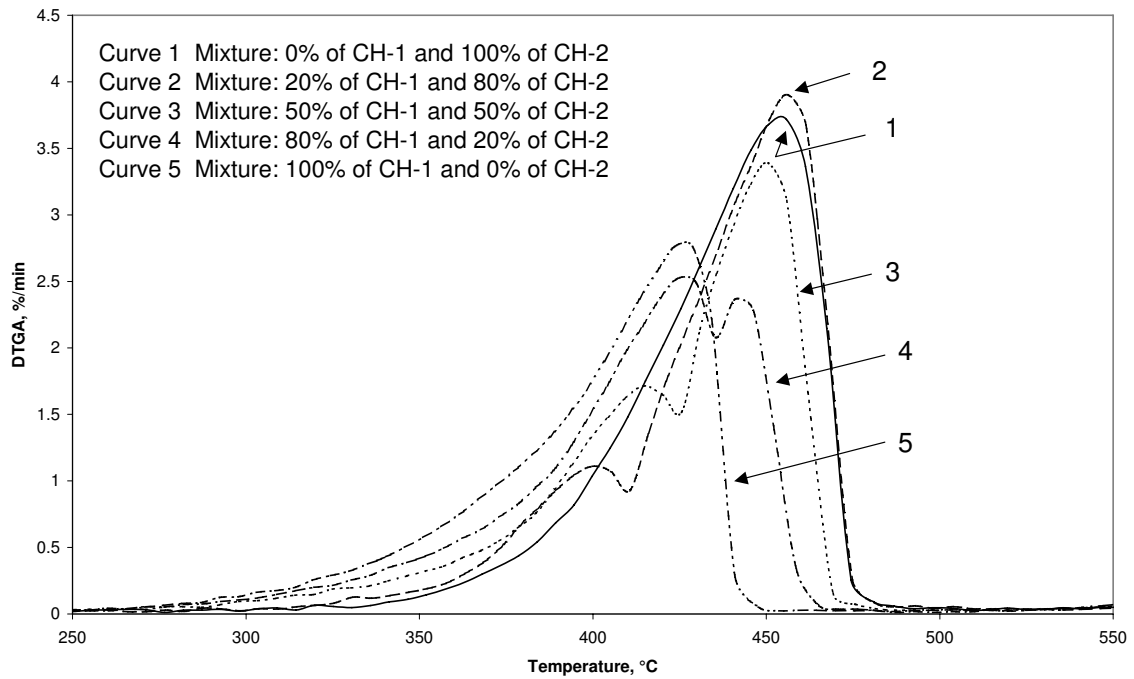


Figure 1 DTGA curves for samples CH-1 and CH-2 and their mixtures with different proportions

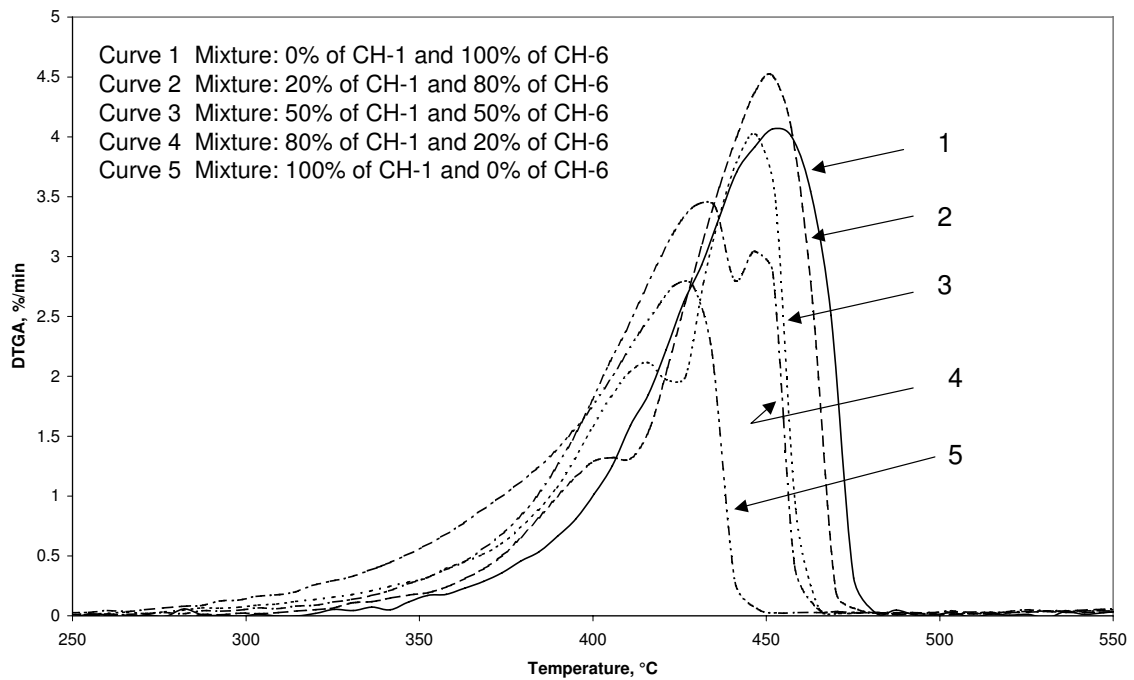


Figure 2 DTGA curves for samples CH-1 and CH-6 and their mixtures with different proportions

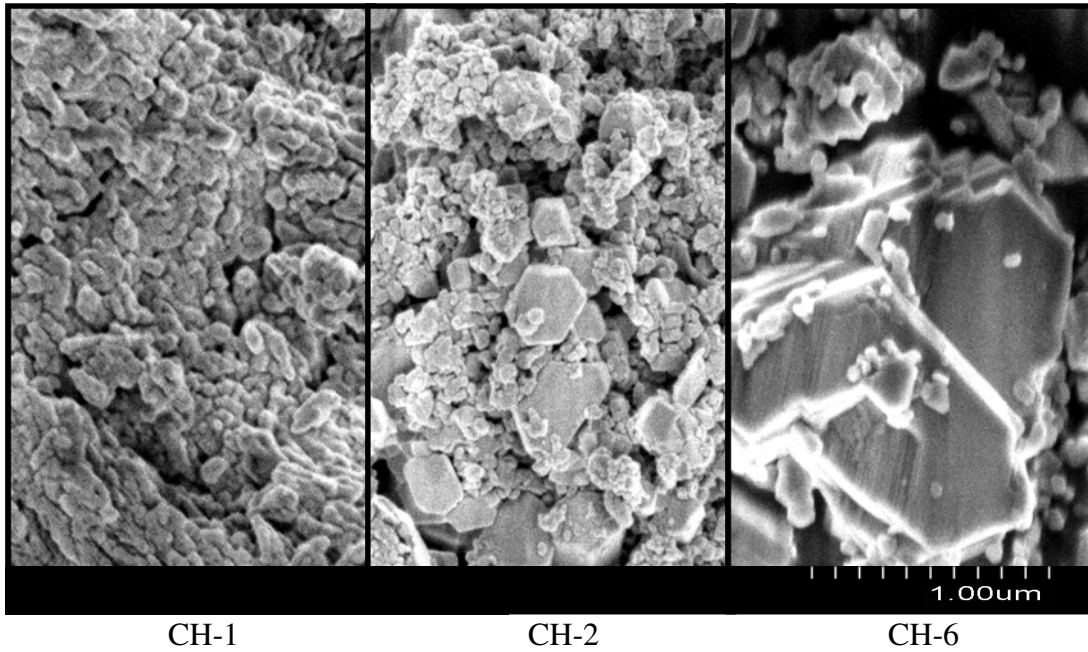


Figure 3 SEM micrographs of CH-1, CH-2 and CH-6

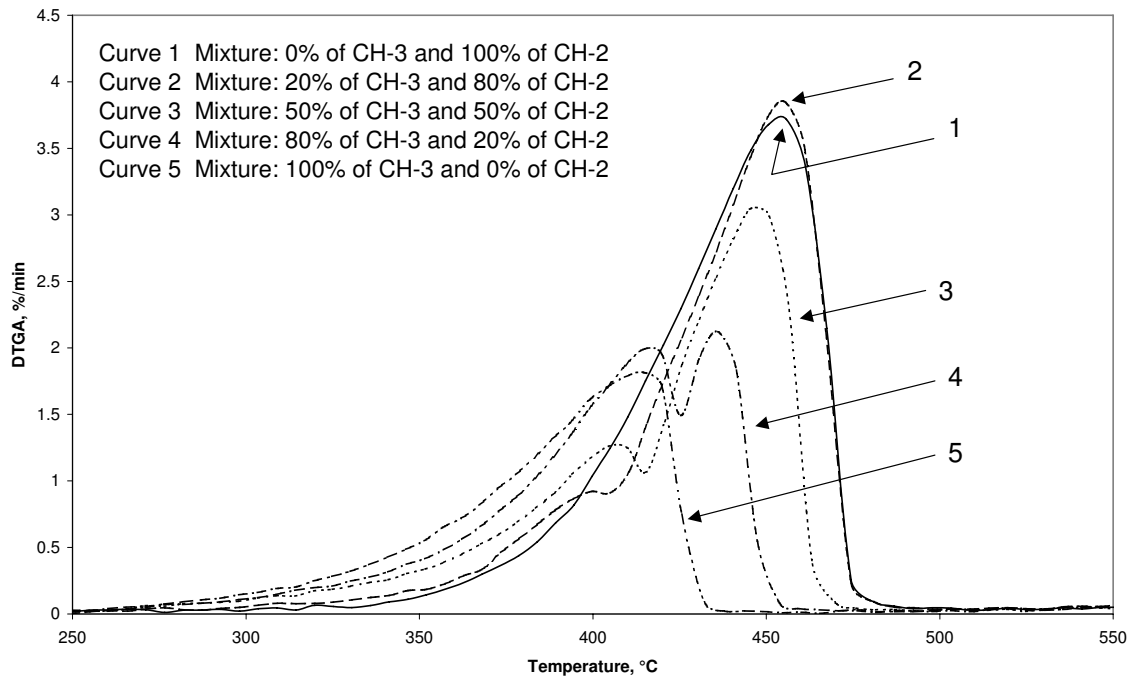


Figure 4 DTGA curves for samples CH-3 and CH-2 and their mixtures with different proportions

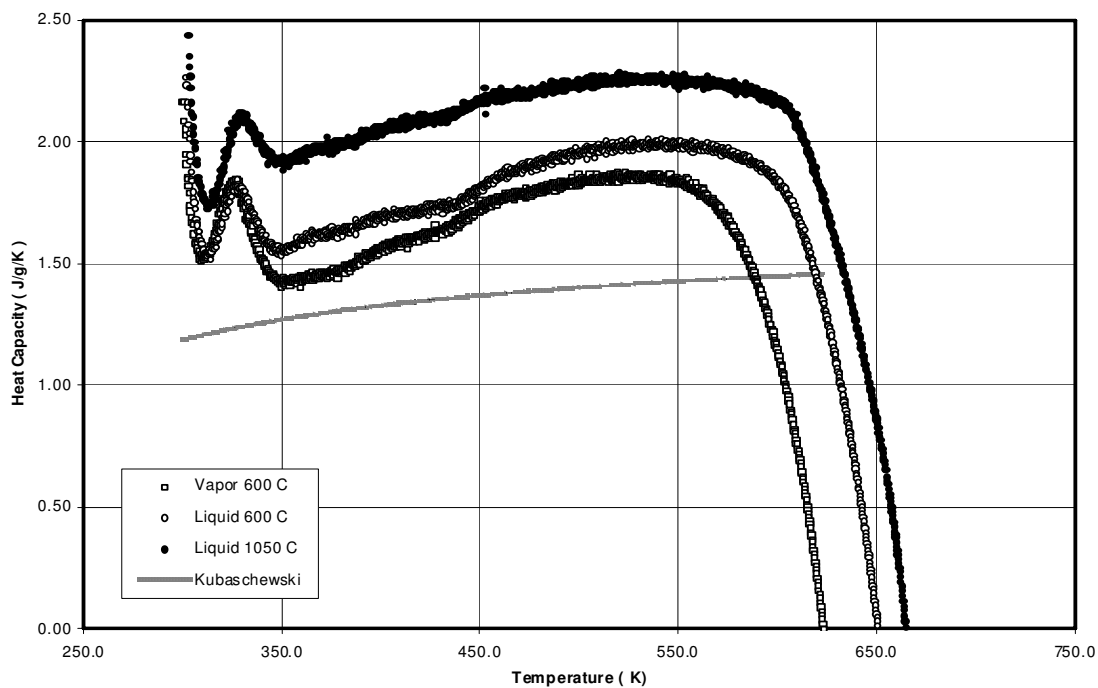


Figure 5 Temperature dependence of heat capacities for $\text{Ca}(\text{OH})_2$ prepared under different conditions

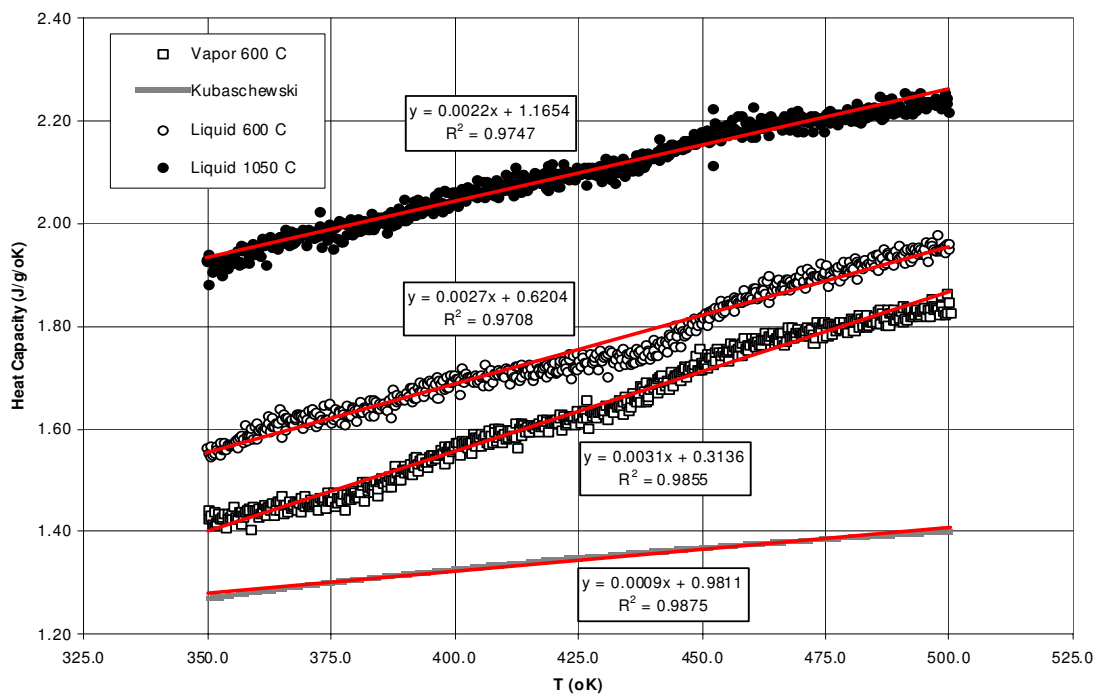


Figure 6 Region of linear temperature dependence for $\text{Ca}(\text{OH})_2$ heat capacities.